



Water-medium C–H activation over a hydrophobic perfluoroalkane-decorated metal-organic framework platform



Yuan-Biao Huang, Min Shen, Xusheng Wang, Ping Huang, Ruiping Chen, Zu-Jin Lin, Rong Cao *

State Key Laboratory of Structural Chemistry, Fujian Institute of Research on the Structure of Matter, Chinese Academy of Sciences, 155, Yangqiao Road West, Fuzhou 350002, China

ARTICLE INFO

Article history:

Received 3 September 2015

Revised 19 October 2015

Accepted 20 October 2015

Keywords:

Metal-organic frameworks

Water-medium

Pd nanoparticles

C–H activation

Perfluoroalkane

ABSTRACT

The use of water as reaction medium in the heterogeneous activation of C–H bonds has numerous advantages in terms of environmental benign, safety and cost efficiency impact. However, it is severely hampered because the reactants are difficult to dissolve in water and contact with the active sites of heterogeneous catalysts. Herein, we choose perfluoroalkane-functionalized mesoporous metal-organic framework (MOF) NU-1000 as a hydrophobic platform to encapsulate ultrafine palladium nanoparticles (Pd NPs) for C–H activation in water. The resultant Pd NPs stabilized by the perfluoroalkane exhibited high activity and regioselectivity in the direct C–H arylation of indoles in water. The introduction of perfluoroalkane chains into the mesoporous pores of NU-1000 provides hydrophobic surfaces to facilitate access of the reactants to the active sites to guarantee the high activity.

© 2015 Elsevier Inc. All rights reserved.

1. Introduction

The C2 arylated indoles are one of the most important building blocks of bioactive molecules [1]. Direct construction of C–C bond from inert C–H bond is a highly efficient and sustainable strategy in the synthesis of arylated indoles due to no need of organometallic activating groups [2–13]. Palladium-catalyzed direct C–H arylations of indoles have been investigated and made great progress over the past few years [2–18]. Unfortunately, the reported direct arylation methodologies were usually carried out in organic solvents, which may be hazardous to health and the environment [16].

The use of heterogeneous catalysts in water-medium C–H activation offers particular environmental and sustainable advantages because water is the most inexpensive and environmentally benign solvent [19–22]. However, most of organometallic catalysts are sensitive to the moisture and the expensive additives, such as Ag salts or phosphine ligands are required. Thus, the catalysis of the C–H arylations of indoles in water-medium with high efficiency remains very challenging [23,24]. Moreover, the active sites in heterogeneous catalysts are not as accessible as those in homogeneous catalysts. In addition, because of its low solubility in water, most organic reactants are difficult to contact with the active centers. Although introduction of co-solvents or surfactants can accelerate reaction rate, the addition of auxiliary additives

leads to difficult to purify the products and has a negative impact on the environment [19]. To overcome these drawbacks, Pd NPs supported on hydrophobic mesoporous materials will provide a promising way for highly efficient catalytic C–H activation in aqueous media. Nevertheless, large surface areas and mesoporous channels are required to guarantee a high dispersion of Pd NPs active sites and facilitate reactants adsorption and diffusion. Meanwhile, hydrophobic materials can enhance the adsorption of hydrophobic organic reactants in aqueous solution, which leads to accelerated reaction rate and enhanced reaction selectivity [20].

MOFs have been emerging as promising heterogeneous catalysts due to their high surface areas, tunable pores and postmodification [25–45]. As known, the perfluoroalkane chains not only can stabilize metal NPs [16,46,47], but also provide hydrophobic environments where the organic substrates could be much more accessible to the active sites in water [48,49]. NU-1000 ($\text{Zr}_6(\mu_3\text{-OH})_8(\text{OH})_8(\text{TBAPy})_2$, TBAPy = 1,3,6,8-tetrakis(p-benzoate)pyrene) has mesopores (3.0 nm) with high thermal stability (up to 500 °C) and chemical stability in boiling water at different pH values (pH = 1–11, Fig. S7) [50], and the eight terminal OH groups on Zr can be used for postmodification with perfluoroalkane chains (Figs. 1 and S1). Therefore, the hydrophobic mesoporous MOFs NU-1000 functionalized with perfluoroalkane chains was selected to immobilize Pd catalyst for the generation of uniform NPs with small size and the enhancement for catalytic activity in water.

Herein, ultrafine Pd NPs were encapsulated in the mesopores of perfluoroalkane functionalized NU-1000 for the high activity in the direct C–H arylation of indoles in water.

* Corresponding author.

E-mail address: rcao@fjirsm.ac.cn (R. Cao).

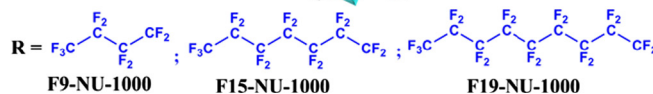


Fig. 1. Schematic representation of introduction of perfluoroalkane chains into the pores of NU-1000 by SALI approach and immobilization of the Pd NPs into the pores of perfluoroalkane functionalized NU-1000 using incipient-wetness impregnation method.

2. Experimental

2.1. Synthesis of perfluoroalkane functionalized NU-1000

The perfluoroalkane functionalized NU-1000 (F9-NU-1000, F15-NU-1000 and F19-NU-1000) was synthesized according to the literature method [51]. 60 mg NU-1000 (0.027 mmol) was loaded in a 10 ml vial. Subsequently a 2.4 ml of 0.1 M solution of fluoroalkane carboxylic acid (0.24 mmol) in DMF was added to the reaction vial, which was then sealed and heated at 60 °C for 24 h with occasional swirling. The supernatant of the reaction mixture was decanted and the MOF sample was soaked into fresh hot DMF which was then filtered, washed sequentially with DMF, acetone and diethyl ether (30, 20 and 15 ml each), and finally dried at 120 °C under vacuum for 12 h. Interestingly, the covalent ester bonds in Fn-NU-1000 cannot be hydrolyzed in boiling water at pH = 1–9 (Fig. S8). Notably, the perfluoroalkanes can be released from the boiling water at pH = 11 for 24 h, while the parent material NU-1000 retains the crystalline structure.

2.2. Preparation of palladium catalysts embedded in NU-1000 and Fn-NU-1000

Pd@NU-1000 and Pd@Fn-NU-1000 ($n = 9, 15$, and 19) were prepared using incipient-wetness impregnation method. Typically, a solution of $\text{Pd}(\text{acac})_2$ (14.5 mg , 0.30 ml CHCl_3) was added dropwise into the activated NU-1000 (or Fn-NU-1000) powder (500 mg) under vigorously stirring in the nitrogen flow. The mixture was continuously stirred for 30 min . The solid was dried at 80°C for 12 h under vacuum and reduced in $5\% \text{ H}_2/\text{N}_2$ flow at 200°C for 3 h . The Pd loading on NU-1000 and Pd@Fn-NU-1000 ($n = 9, 15$, and 19) was 1.14 wt\% , 0.98 wt\% , 1.20 wt\% and 1.11 wt\% , respectively, according to the ICP.

2.3. Catalytic test

Typically, 1.0 ml H₂O was added into the mixture of indole (1.0 mmol), aryl halide (1.2 mmol), KOAc (3.0 mmol), and the palladium catalyst (1.0 mol% Pd). The reaction mixture was stirred at 100 °C for 24 h. After cooling to room temperature, most of the products are present in the aqueous phase. The suspension was centrifuged. To completely collect the products residual remaining in the solid NU-1000, ethyl acetate was used to wash for three times (5 ml × 3). The aqueous phase was extracted three times using ethyl acetate (5 ml × 3). The two parts of organic phase were combined and subsequently washed with water and brine and then dried over Na₂SO₄. The product was purified by silica gel chromatography (mixture of light petroleum and ethyl acetate as

eluent). The identification was conducted by ^1H and ^{13}C NMR measurement.

For the measurement of the Pd leaching during the reaction, a hot-filtration experiment was run to investigate whether the reaction proceeded in a heterogeneous or homogeneous fashion. After 6 h, the catalyst was separated by hot filtration and the filtrate was further treated under the same conditions for another 42 h. For the recyclability test, the catalyst was recovered from each of the reaction of *N*-methylindole with iodobenzene at 100 °C for 24 h, washed with water and acetone several times, and then dried under vacuum at 150 °C for the next use.

3. Results and discussion

3.1. Preparation and characterization of catalysts

NU-1000 was synthesized and purified according to the literature [50]. A series of perfluoroalkanes with different chain length decorated in the mesoporous channels of NU-1000, denoted as Fn-NU-1000 (e.g., F9-NU-1000, F15-NU-1000 and F19-NU-1000) was easily obtained using solvent-assisted ligand incorporation (SALI) approach (Figs. 1 and S1) [51]. Here n is the number of the fluorine atoms in the perfluoroalkanes chains. After digestion with D_2SO_4 , ^{19}F NMR spectra of the functionalized NU-1000 proved the successful decoration with perfluoroalkanes (Figs. S2–S4). The powder X-ray diffraction (PXRD) patterns of the obtained yellow solids are coincident with that of the simulated NU-1000, confirming that the functionalized samples retain their crystallinity (Fig. S5). The N_2 adsorption measurements (Fig. 2a and Table S1) showed a large specific surface areas ($S_{\text{BET}} = 2742.6 \text{ m}^2 \text{ g}^{-1}$) of the obtained NU-1000 [50,51]. Interestingly, although the samples Fn-NU-1000 exhibited lower specific surface areas (Fig. 2a), they still remain mesoporous after functionalized with fluoroalkane chains (Table S1), which cannot prevent the loading of Pd catalysts. More interestingly, compared to NU-1000, all the fluoroalkanes functionalized samples showed lower water uptakes with increasing fluoroalkane chain length (Fig. 2b), which indicated the mesopores become hydrophobic platforms [51].

Pd NPs embedded in NU-1000 and Fn-NU-1000 (here denoted as Pd@NU-1000 and Pd@Fn-NU-1000, $n = 9, 15$, and 19) were prepared using incipient-wetness impregnation method, followed by treatment with H_2 at $200\text{ }^\circ\text{C}$ for 3 h . The PXRD patterns (Fig. S6) show that there is no significant loss of crystallinity, and no supplementary Bragg peaks appearance, which indicated that the integrity of the frameworks of the MOFs was maintained after the Pd loading. Moreover, the characteristic peak of Pd was indistinguishable indicating the formation of small Pd NPs [30]. Compared with the corresponding bare supports, the obvious decreases in the surface areas of Pd@NU-1000, Pd@Fn-NU-1000

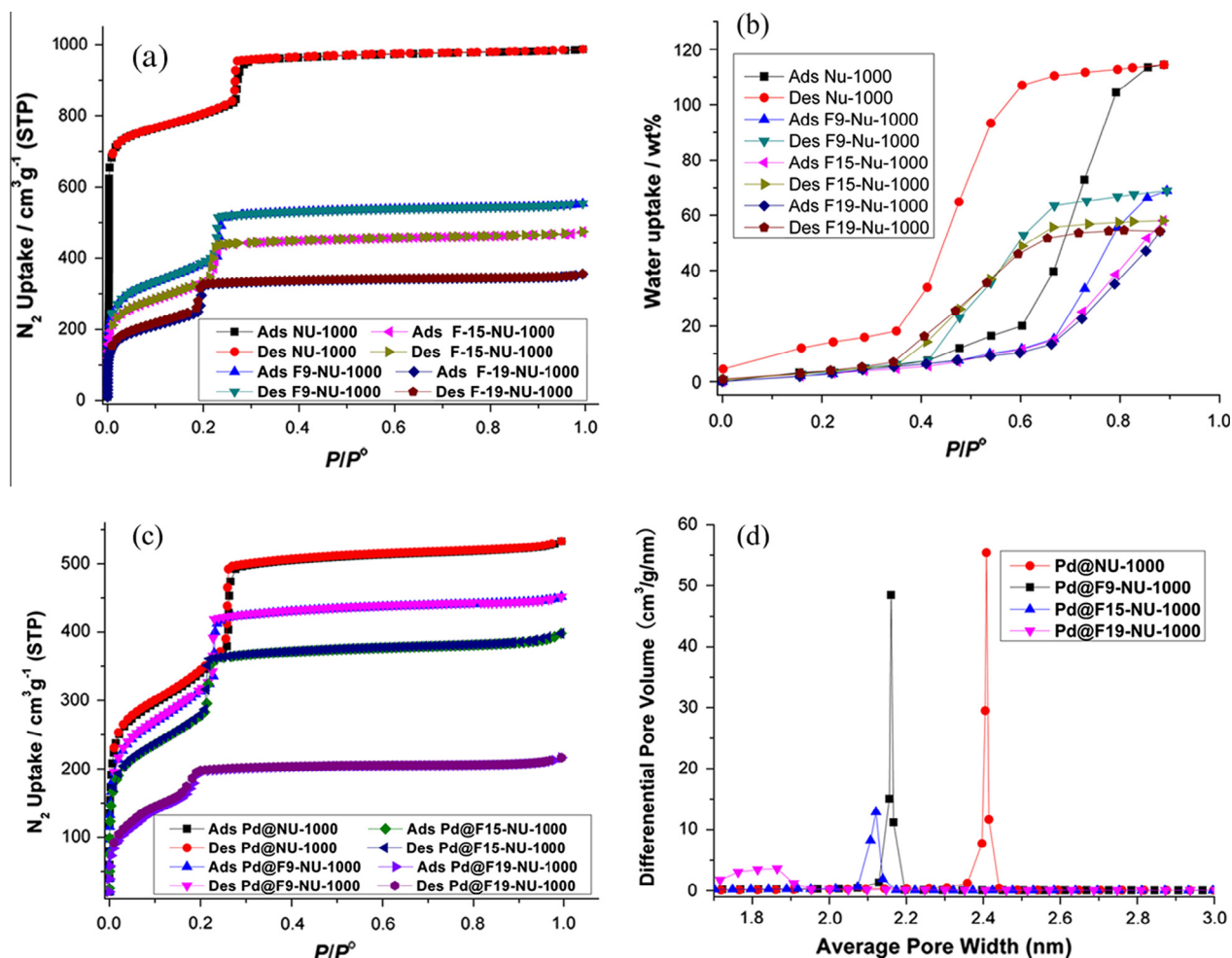


Fig. 2. (a) Nitrogen sorption isotherms at 77.3 K for NU-1000 and Fn-NU-1000 samples. (b) Water isotherms of NU-1000 and Fn-NU-1000 samples at 298 K; P° is the saturated vapor pressure at 298 K. (c) Nitrogen sorption isotherms at 77.3 K for Pd@NU-1000 and Pd@Fn-NU-1000 samples. (d) BJH pore size distributions for Pd@NU-1000 and Pd@Fn-NU-1000 samples.

indicate that the pores of the host frameworks were occupied by dispersed Pd NPs (Figs. 2a, c, and S9, Table S1) [30]. Interestingly, although a slight decrease of the pore sizes after the incorporations of Pd NPs, all the MOFs composites are in the mesoporous ranges except Pd@F19-NU-1000 functionalized with the long fluoroalkane chains (Fig. 2d and Table S1). Therefore, the substrates still can access into the catalytic active sites through the mesoporous windows.

X-ray photoelectron spectroscopy (XPS) spectra (Fig. S11) show that the $3d^{5/2}$ and $3d^{3/2}$ peaks of Pd appear at 335.77 and 341.14 eV, respectively, which indicates that most of the palladium is in the reduced form [32]. It should be noted that the weak intensity of the Pd peaks is due to the low ratio of the Pd/Zr (1.20 wt% Pd, Fig. S13). The other two peaks at 347.29 and 333.85 eV are ascribed to the Zr $3p^{1/2}$ and Zr $3p^{3/2}$, respectively, while the Zr 3d peaks for Zr $3d^{5/2}$ and Zr $3d^{3/2}$ are located at 182.78 eV and 185.17 eV, respectively.

Transmission electron microscopy (TEM) (Figs. 3a and S12), high-annular dark-field scanning TEM (HAADF-STEM) images (Figs. 3b and S13–S15) and HRTEM images (Fig. 3c) of Pd@Fn-NU-1000 and Pd@NU-1000 show that the uniformly dispersed Pd NPs are formed. Combined with the preparation method, N_2 adsorption results and TEM images, it can be deduced that most of the Pd NPs are embedded in the pores of Fn-NU-1000 and NU-1000, although a few of the particles are found on the outside

surface. The average particle size is very small (ca. 2.5 nm, Fig. 3d), which could be ascribed to the confinement of the mesopores of F15-NU-1000 [44] and the entrapment of the perfluoroalkane chains [48,49]. Interestingly, TEM images (Figs. 3a and S12) and HAADF-STEM images (Fig. 3b) show the average adjacent lattice plane of Pd@F15-NU-1000 is ca. 2.74 nm (7 of lattice fringes are 19.18 nm), which implies that the structural integrity of F15-NU-1000 was preserved after the Pd incorporation. It further proved that NU-1000 functionalized with fluoroalkane chains was indeed stable even under the irradiation of the TEM electron beam.

3.2. C–H arylation of indoles

It is well known that C–H arylation of free indole is more difficult than the *N*-substituted derivatives. Therefore, the free indole and iodobenzene were employed as the substrates in the screening of optimized reaction conditions in water. All the reactions were performed in the air atmosphere and C2-arylation products were obtained as the major regioisomers. Gratifyingly, the good GC yield (81.3%) and high selectivity (C2/C3 = 22.4, the ratio of the C2 product and C3 product) were obtained when using 1.0 mol% Pd catalyst Pd@F15-NU-1000 at 100 °C after 24 h (Tables S2–S4 and Fig. S16). In contrast, higher catalyst loadings (5 mol%) are generally required in the homogeneous catalyst system even in the organic solvents [19,20]. Although increasing the amount of

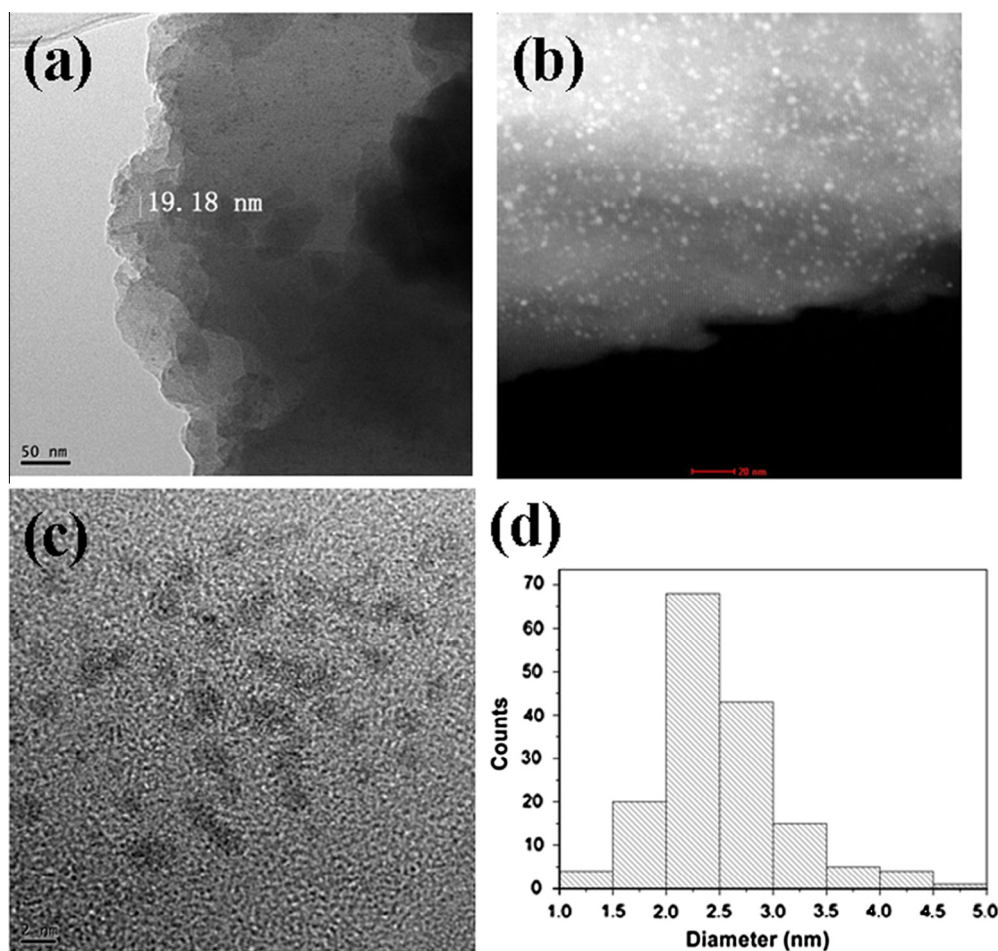


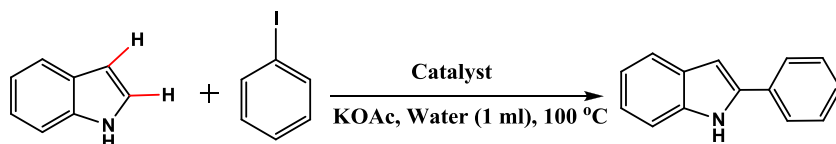
Fig. 3. (a) TEM, (b) HAADF-STEM, (c) HRTEM images of Pd@F15-NU-1000 and (d) the size distribution of Pd NPs. Scale bars = 50, 20, 2 nm in (a), (b) and (c), respectively.

the catalyst to 2.0 mol% Pd led to a little higher yield, the selectivity of C2/C3 decreased and a small amount of the by-product biphenyl was produced (Table S4, entry 5).

As we expected, different perfluoroalkane chain length plays a vital role in the catalysis in water. Although the mesoporous NU-1000 has higher surface area and pore volumes, unfortunately, it exhibited lower activity (Table 1, entry 1). It can be ascribed to that

the hydrophilic pore environment inhibits the diffusion of the organic substrates into the Pd active sites in water [49]. Interestingly, perfluoroalkane chains functionalized catalysts efficiently enhanced the C–H activation in water (Table 1, entries 2–4). Pd@F9-NU-1000 gave approximately twice yields (Table 1, entry 2) than the nonfunctionalized catalyst (Table 1, entry 1). Satisfactorily, longer perfluoroalkane chains decorated Pd@F15-NU-1000

Table 1
Direct arylation of indole in water with different Pd catalysts.^a



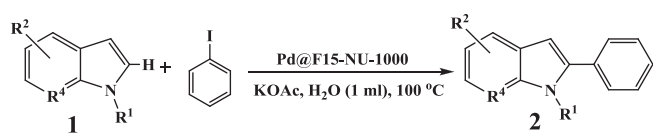
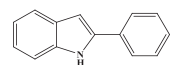
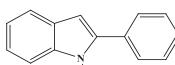
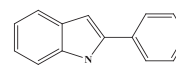
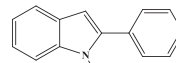
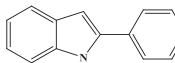
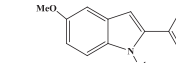
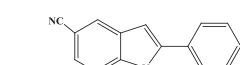
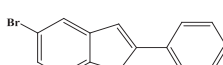
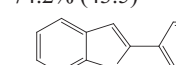
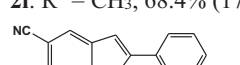
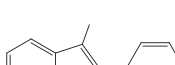
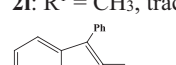
Entry	Pd-based catalyst (wt% Pd)	Yield (%) ^b	Selectivity (C2/C3) ^c
1	Pd@NU-1000 (1.14)	12.5	9.3
2	Pd@F9-NU-1000 (0.98)	24.3	11.1
3	Pd@F15-NU-1000 (1.20)	87.2	21.1
4	Pd@F19-NU-1000 (1.11)	84.2	20.3
5	Pd(acac) ₂ @F15-NU-1000 (1.00)	11.1	6.3
6	Pd@MIL-101(Cr) (0.56)	33.7	19
7	Pd/MIX-MIL-53(Al) (1.53)	27.1	15

^a Conditions: 1.0 mmol indole, 1.2 mmol iodobenzene, Pd-based catalyst (1.0 mol% Pd), KOAc (3 mmol), air, 48 h.

^b GC yield.

^c Selectivity determined by GC–MS

Table 2Direct arylation of various indoles with PhI.^a

		
 2a: 77.3% (22.3)	 2b: trace	 2c: trace
 2d: 73.4% (19.7)	 2e: 66.7% (11.2)	 2f: R ¹ = H, 72.1% ^b (33.4); 2g: R ¹ = CH ₃ , 74.2% (43.5)
 2h: R ¹ = H, 61.2% ^b (21.1); 2i: R ¹ = CH ₃ , 68.4% (17.7)	 2j: 76.3% ^b (32.2)	 2k: R ¹ = H, trace; 2l: R ¹ = CH ₃ , trace
 2m: trace	 2n: no product	 2o: 6.5% ^b

^a Conditions: 1.0 mmol indole derivatives, 1.2 mmol iodobenzene, Pd@F15-NU-1000 (1.0 mol% Pd), KOAc (3 mmol), air, 24 h. Isolated yields of pure C2-isomers after flash column chromatography are reported. Values in brackets refer to C2/C3 selectivity of the product determined by GC–MS.

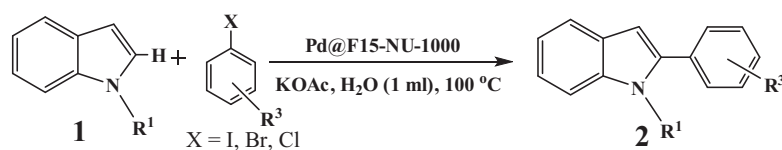
^b GC yield.

gained high activity (87.1%) and selectivity (21.1, Table 1, entry 3). Although Pd@F19-NU-1000 with longer chains showed a little lower activity to the lower surface areas and pore volumes (Fig. 2c and Table S1), it also gave 84.2% yield. These findings are associated with that the water adsorption uptakes decrease from a shorter to longer perfluoroalkane chains (Fig. 2b). It indicated that the introduction of perfluoroalkane chains not only provides hydrophobic inner surfaces to facilitate access of the organic reactants to the active sites, but also inhibits the migration and aggregation of Pd NPs in the reduction and catalysis processes. Furthermore, the catalyst Pd@F15-NU-1000 still possesses larger surface areas and accessible mesoporous pores, which ensures the high dispersion of the active sites and facilitates the diffusion of the substrates in the pores. Other supported palladium catalysts also proved the results (Table 1, entries 6–7). Pd NPs supported on the hydrophilic mesocages of MIL-101(Cr) [14,15] gave only 33.7% yield (Table 1, entry 6), although it has large surface areas and pore volumes. The microporous (0.86 nm) mixed-linker MOF MIX-MIL-53(Al) (Al(OH)[BDC]_x[H₂N-BDC]_{1-x}) containing free amine group shows high thermal stability [52]. Well-dispersed palladium nanoparticles (Pd NPs, 3.2 nm) supported on MIX-MIL-53(Al) (Pd/MIX-MIL-53(Al)) were easily obtained using the ion-exchange method, which showed high activity for Heck reactions [52]. However, a poor activity was also observed in the catalyst Pd/MIX-MIL-53(Al) (the ratio of the ligands is $x = 0.5$) (Table 1, entry 7) due to the hydrophilic microporous channels [52].

A hot filtration experiment was performed to confirm the heterogeneity of the catalyst. After the reaction was performed 6 h, Pd@F15-NU-1000 catalyst was separated by hot filtration and the filtrate was monitored under identical reaction conditions

for another 42 h. As expected, no further conversion was detected after the removal of Pd@F15-NU-1000 (Fig. S16). After the workup, there was no detectable Pd leaching into the filtrate by the inductively coupled plasma atomic emission spectroscopy (ICP–AES) analysis. Interestingly, after recycled for six runs of the reaction of *N*-methylindole and iodobenzene, the Pd catalyst still exhibited high activity (Fig. S17). The PXRD patterns revealed that the crystalline structure of the catalyst was still retained after six catalytic cycles (Fig. S6). In addition, there was no Pd peak appearing in the PXRD, which indicated that there was no aggregation of Pd NPs during the reaction. Impressively, indeed, the TEM images of the catalyst after six catalytic recycles showed that the size of Pd NPs was similar to that before reaction (Mean size = 2.53 nm, Fig. S18). The result may be contributed to that the Pd NPs are confined into the pores of F15-NU-1000 and entrapped by the perfluoroalkane chains. The N₂ sorption results exhibit that the Pd@F15-NU-1000 catalyst still remained porous with high surface area ($S_{\text{BET}} = 975.9 \text{ m}^2 \text{ g}^{-1}$) and pore size (2.09 nm) after six catalytic cycles (Fig. S19). In contrast, the Pd²⁺ counterparts Pd(acac)₂ supported on F15-NU-1000 (Pd(acac)₂@F15-NU-1000) showed low activity and selectivity of the C2 arylation product (Table 1, entry 5). The TEM of Pd(acac)₂@F15-NU-1000 after catalysis (Fig. S20) indicated that larger NPs (11.1 nm) were in situ formed, which were difficult to activate the substrates effectively. Thus, according to these results, the reaction occurs in a heterogeneous fashion, although it cannot completely exclude that the leached active Pd species redeposited in the support after the coupling reaction [53].

Subsequently, the scope of the reaction was evaluated for a series of indole and aryl iodide derivatives (Tables 2 and 3). The substituents on the *N* atom of indoles affect dramatically the activity

Table 3
Direct arylation of various indoles with aryl halides.^a

Entry	R ³	Product	Yield (%) ^b selectivity ^c
1 ^d	H		Trace
2 ^d	H		Trace
3	H		77.3% (22.3)
4	H		73.4 (19.7)
5	4-Br		78.2% (26.3)
6	4-Me		81.2 (22.3)
7	4-Me		78.3 (19.4)
8	4-CF ₃		76.8 (17.4)
9	4-CF ₃		74.1 (16.2)

^a Conditions: 1.0 mmol indole derivatives, 1.2 mmol aryl iodides (except entries 1 and 2 using bromides and chlorides, respectively), Pd@F15-NU-1000 (1.0 mol% Pd), KOAc (3 mmol), air, 24 h.

^b Isolated yield.

^c Values in brackets refer to C2/C3 selectivity of the product determined by GC–MS.

^d 48 h, X = Br (Cl), 1.2 mmol.

(Table 2). Interestingly, the free *N*-H indole obtained a high isolated yield of **2a** (77.3%) and selectivity (22.3). It should be noteworthy that the same reaction catalyzed by Pd/MIL-101 at 120 °C afforded only 18% yield of the desired C2 product in the organic solvent [14]. Although the indole derivatives on the *N* atoms with electron-withdraw groups (Ac for **2b** and Boc for **2c**) cannot be effectively activated, the electron-donating groups substituted indoles gave high yields and selectivities of the C2 arylated products (**2d** and **2e**). The results indicated a support for the electrophilic palladation mechanism [6]. In addition, the electron-donating substituents on the phenyl segment of the free *N*-H indole and *N*-methylindole gave better yields (72.1–74.2%) and selectivities (Table 2f–g) than the corresponding substrates containing electron-withdraw groups (Table 2h–i). It should be noted that C–Br bond of bromoindole can be tolerated, affording a high isolated yield (76.3%) and chemoselectivity (32.2, **2j**), which allows further functionalization through cross coupling reactions. Unfortunately, replacing the benzene ring of indole or *N*-methylindole with the pyridine group resulted in no arylation (**2k–2m**), which may be ascribed to that Pd NPs are easily coordinated with the pyridine groups in water [23]. 3-Methylindole

cannot be activated to obtain the C2 arylation product (**2n**), while 2-methylindole can afford to a small amount of C3 arylation product (**2o**), which indicates that a C3-to-C2 migration of Pd may take place during the reaction [6]. Notably, the lower activity and selectivity of the substrate functionalized with bulky substituent on the *N* atoms also support a C3-to-C2 migration of Pd mechanism [6].

The effects of a variety of substituted aryl halides were also examined (Table 3). It was not surprised that the reaction of bromobenzene/chlorobenzene with free *N*-H indole or *N*-methylindole afforded to traces of C2 arylation products due to the difficult activation of the C–Br and C–Cl bonds with high bond energy (Table 3, entries 1 and 2). These findings have been found in other Pd (OAc)₂-catalyzed homogeneous catalysis in organic solvents [6,7]. Interestingly, the C–Br bond was tolerated when 1-bromo-4-iodobenzene reacted with free *N*-H indole to obtain **2p**, which can be further functionalized (Table 3, entry 5). Furthermore, the reactions proceeded extraordinarily well with a variety of substituted iodobenzenes, with indole or *N*-methylindole, giving C2-arylation products (2q–2t) in good yields and selectivities (Table 3, entries 9).

4. Conclusions

In conclusion, we developed a sustainable heterogeneous catalyst for the direct C–H arylation of indoles in water using ultrafine Pd NPs, which embedded in the hydrophobic mesoporous pores of NU-1000 decorated with perfluoroalkanes. The methodology was found to be general, and provided the desired C2-arylindoles with high yields and regioselectivities. Notably, it was no need of the expensive additives Ag_2CO_3 base or phosphine ligands, and co-solvents or surfactants. More importantly, the catalyst can be easily recoverable and reused for several times without leaching and loss of activity. This study offers a novel approach to synthesize organic molecules, which affords economical, environmental benign and safety advantages.

Acknowledgments

The authors thank Prof. Weiping Su for the valuable suggestions. We acknowledge the financial support from the 973 Program (2011CB932504 and 2013CB933200), NSFC (21273238, 21221001, 21331006 and 21303025), the NSF of Fujian Province (2014J05022 and 2014J05020), Chunmiao Project of Haixi Institute of Chinese Academy of Sciences (CMZX-2014-004) and Youth Innovation Promotion Association, CAS (2014265).

Appendix A. Supplementary material

Supplementary data associated with this article can be found, in the online version, at <http://dx.doi.org/10.1016/j.jcat.2015.10.012>.

References

- [1] S. Cacchi, G. Fabrizi, *Chem. Rev.* 105 (2005) 2873.
- [2] R.Y. Tang, G. Li, J.Q. Yu, *Nature* 507 (2014) 215.
- [3] D.R. Stuart, K. Fagnou, *Science* 316 (2007) 1172.
- [4] S.H. Cho, J.Y. Kim, J. Kwak, S. Chang, *Chem. Soc. Rev.* 40 (2011) 5068.
- [5] M. Platon, R. Amardeil, L. Djakovitch, J.-C. Hierso, *Chem. Soc. Rev.* 41 (2012) 3929.
- [6] B.S. Lane, M.A. Brown, D. Sames, *Am. Chem. Soc.* 127 (2005) 8050.
- [7] N. Lebrasseur, I. Larrosa, *J. Am. Chem. Soc.* 130 (2008) 2926.
- [8] S. Potavathri, K.C. Pereira, S.I. Gorelsky, A. Pike, A.P. LeBris, B. DeBoef, *J. Am. Chem. Soc.* 132 (2010) 14676.
- [9] S.-D. Yang, C.-L. Sun, Z. Fang, B.-J. Li, Y.-Z. Li, Z.-J. Shi, *Angew. Chem. Int. Ed.* 47 (2008) 1473.
- [10] S. Kirchberg, R. Fröhlich, A. Studer, *Angew. Chem. Int. Ed.* 48 (2009) 4235.
- [11] S. Kirchberg, R. Fröhlich, A. Studer, *Angew. Chem. Int. Ed.* 49 (2010) 6877.
- [12] N.R. Deprez, D. Kalyani, A. Krause, M.S. Sanford, *J. Am. Chem. Soc.* 128 (2006) 4972.
- [13] M. Conte, C.J. Davies, D.J. Morgan, T.E. Davies, D.J. Elias, A.F. Carley, P. Johnston, G.J. Hutchings, *J. Catal.* 297 (2013) 128.
- [14] Y. Huang, Z. Lin, R. Cao, *Chem. Eur. J.* 17 (2011) 12706.
- [15] Y. Huang, T. Ma, P. Huang, D. Wu, Z. Lin, R. Cao, *ChemCatChem* 5 (2013) 1877.
- [16] L. Wang, W.B. Yi, C. Cai, *Chem. Commun.* 47 (2011) 806.
- [17] J. Malmgren, A. Nagendiran, C.-W. Tai, J.-E. Bäckvall, B. Olofsson, *Chem. Eur. J.* 20 (2014) 13531.
- [18] L. Djakovitch, F.-X. Felpin, *ChemCatChem* 6 (2014) 2175.
- [19] C.I. Herrerías, X. Yao, Z. Li, C.-J. Li, *Chem. Rev.* 107 (2007) 2546.
- [20] M.-O. Simon, C.-J. Li, *Chem. Soc. Rev.* 41 (2012) 1415.
- [21] B. Li, P.H. Dixneuf, *Chem. Soc. Rev.* 42 (2013) 5744.
- [22] G.L. Turner, J.A. Morris, M.F. Greaney, *Angew. Chem. Int. Ed.* 46 (2007) 7996.
- [23] L. Joucla, N. Batail, L. Djakovitch, *Adv. Synth. Catal.* 352 (2010) 2929.
- [24] S. Islam, I. Larrosa, *Chem. Eur. J.* 19 (2013) 15093.
- [25] J. Liu, L. Chen, H. Cui, J. Zhang, L. Zhang, C.-Y. Su, *Chem. Soc. Rev.* 43 (2014) 6011.
- [26] M. Yoon, R. Srirambalaji, K. Kim, *Chem. Rev.* 112 (2012) 1196.
- [27] A. Corma, H. García, L.F.X.i. Xamena, *Chem. Rev.* 110 (2010) 4606.
- [28] Q.-L. Zhu, Q. Xu, *Chem. Soc. Rev.* 43 (2014) 5468.
- [29] C. Rösler, R.A. Fischer, *CrystEngComm* 17 (2015) 199.
- [30] J. Juan-Alcañiz, J. Ferrando-Soria, I. Luz, P. Serra-Crespo, E. Skupien, V.P. Santos, E. Pardo, L.F.X.i. Xamena, F. Kapteijn, J. Gascon, *J. Catal.* 307 (2013) 295.
- [31] E.V. Ramos-Fernandez, C. Pieters, B. van der Linden, J. Juan-Alcañiz, P. Serra-Crespo, M.W.G.M. Verhoeven, H. Niemantsverdriet, J. Gascon, F. Kapteijn, *J. Catal.* 289 (2012) 42.
- [32] X. Jia, S. Wang, Y. Fan, *J. Catal.* 327 (2015) 54.
- [33] N.T.T. Tran, Q.H. Tran, T. Truong, *J. Catal.* 320 (2014) 9.
- [34] A. Dhakshinamoorthy, H. Garcia, *Chem. Soc. Rev.* 41 (2012) 5262.
- [35] A. Dhakshinamoorthy, A.M. Asiric, H. Garcia, *Chem. Commun.* 50 (2014) 12800.
- [36] B. Yuan, Y. Pan, Y. Li, B. Yin, H. Jiang, *Angew. Chem. Int. Ed.* 49 (2010) 4054.
- [37] H. Li, Z. Zhu, F. Zhang, S. Xie, H. Li, P. Li, X. Zhou, *ACS Catal.* 1 (2011) 1604.
- [38] G.H. Dang, T.T. Dang, D.T. Le, T. Truong, N.T.S. Phan, *J. Catal.* 319 (2014) 258.
- [39] Q. Yang, Y.-Z. Chen, Z.U. Wang, Q. Xu, H.-L. Jiang, *Chem. Commun.* 51 (2015) 10419.
- [40] M. Zhao, K. Deng, L. He, Y. Liu, G. Li, H. Zhao, Z. Tang, *J. Am. Chem. Soc.* 136 (2014) 1738.
- [41] Y. Huang, S. Liu, Z. Lin, W. Li, X. Li, R. Cao, *J. Catal.* 292 (2012) 111.
- [42] K. Manna, T. Zhang, F.X. Greene, W. Lin, *J. Am. Chem. Soc.* 137 (2015) 2665.
- [43] D. Feng, K. Wang, J. Su, T.-F. Liu, J. Park, Z. Wei, M. Bosch, A. Yakovenko, X. Zou, H.-C. Zhou, *Angew. Chem. Int. Ed.* 54 (2015) 149.
- [44] G. Lu, S. Li, Z. Guo, O.K. Farha, B.G. Hauser, X. Qi, Y. Wang, X. Wang, S. Han, X. Liu, J.S. DuChene, H. Zhang, Q. Zhang, X. Chen, J. Ma, S.C.J. Loo, W.D. Wei, Y. Yang, J.T. Hupp, F. Huo, *Nature Chem.* 19 (2012) 1272.
- [45] P. Wang, J. Zhao, X. Li, Y. Yang, Q. Yang, C. Li, *Chem. Commun.* 49 (2013) 3330.
- [46] M. Tristany, B.P. Chaudret, P. Dieudonné, Y. Guari, P. Lecante, V. Matsura, M. Moreno-Mañas, K. Philippot, R. Pleixats, *Adv. Funct. Mater.* 16 (2006) 2008.
- [47] M. Tristany, J. Courmarcel, P. Dieudonné, M. Moreno-Mañas, R. Pleixats, A. Rimola, M. Sodupe, S. Villarroja, *Chem. Mater.* 18 (2006) 716.
- [48] S. Minakata, M. Komatsu, *Chem. Rev.* 109 (2009) 711.
- [49] H. Shintaku, K. Nakajima, M. Kitano, M. Hara, *Chem. Commun.* 50 (2014) 13473.
- [50] J.E. Mondloch, W. Bury, D. Fairen-Jimenez, S. Kwon, E.J. DeMarco, M.H. Weston, A.A. Sarjeant, S.T. Nguyen, P.C. Stair, R.Q. Snurr, O.K. Farha, J.T. Hupp, *J. Am. Chem. Soc.* 135 (2013) 10294.
- [51] P. Deria, J.E. Mondloch, E. Tylianakis, P. Ghosh, W. Bury, R.Q. Snurr, J.T. Hupp, O. K. Farha, *J. Am. Chem. Soc.* 135 (2013) 16801.
- [52] Y. Huang, S. Gao, T. Liu, J. Lü, X. Lin, H. Li, R. Cao, *ChemPlusChem* 77 (2012) 106.
- [53] P. Fang, A. Jutand, Z. Tian, C. Amatore, *Angew. Chem. Int. Ed.* 50 (2011) 12184.